A MODAL APPROACH TO THE NUMERICAL SIMULATION OF A STRING VIBRATING AGAINST AN OBSTACLE: APPLICATIONS TO SOUND SYNTHESIS

Clara Issanchou, Jean-Loïc Le Carrou, Stefan Bilbao, Cyril Touzé, Olivier Doaré

A MODAL APPROACH TO THE NUMERICAL SIMULATION OF A STRING VIBRATING AGAINST AN OBSTACLE: APPLICATIONS TO SOUND SYNTHESIS

Clara Issanchou, Jean-Loïc Le Carrou
CNRS, LAM / d'Alembert
Sorbonne Universités, UPMC Univ Paris 06
Paris, France
issanchou@lam.jussieu.fr

Stefan Bilbao
Acoustics and Audio Group
University of Edingurgh
Edinburgh, Scotland
sbilbao@staffmail.ed.ac.uk

Cyril Touzé, Olivier Doaré
IMSIA, ENSTA ParisTech-CNRS-EDF-CEA
Université Paris Saclay
Palaiseau, France
cyril.touze@ensta-paristech.fr

ABSTRACT

A number of musical instruments (electric basses, tanpuras, sitars...) have a particular timbre due to the contact between a vibrating string and an obstacle. In order to simulate the motion of such a string with the purpose of sound synthesis, various technical issues have to be resolved. First, the contact phenomenon, inherently nonlinear and producing high frequency components, must be described in a numerical manner that ensures stability. Second, as a key ingredient for sound perception, a fine-grained frequency-dependent description of losses is necessary. In this study, a new conservative scheme based on a modal representation of the displacement is presented, allowing the simulation of a stiff, damped string vibrating against an obstacle with an arbitrary geometry. In this context, damping parameters together with eigenfrequencies of the system can be adjusted individually, allowing for complete control over loss characteristics. Two cases are then numerically investigated: a point obstacle located in the vicinity of the boundary, mimicking the sound of the tanpura, and then a parabolic obstacle for the sound synthesis of the sitar.

1. INTRODUCTION

In many musical instruments, across various cultures, the interaction between a vibrating structure and an obstacle is a key feature leading to amplitude-dependent timbral modification, and is essential in order to replicate the resulting sound. This contact may arise due to the excitation of the instrument [1, 2], in which case the exciting mechanism may be considered as lumped, or during its consequent vibrations [3]. In the latter case, the contact can be pointwise (e.g. the case of string/fret contact in an electric bass) or distributed (e.g. string/bridge contact in a sitar). Such interactions are strongly nonlinear, which complicates significantly its numerical study.

Following analytical studies of the contact between a string and a rigid obstacle [4, 5, 6], a number of numerical methods have been developed in order to simulate the interaction between a vibrating string and an obstacle. Waveguides are used in [7, 8, 9, 10], coupled with finite difference schemes in [11], where the string is ideal, and [12], where the string is damped and stiff and the obstacle is located at one end of the string. A modal description is presented in [13] for modelling an ideal string vibrating against a parabolic obstacle at one boundary and in [14] for a dispersive lossy string where an obstacle consolidated at the bridge of a tanpura is considered. This instrument is also modelled in [15, 16], where the motion of a stiff damped string against an obstacle is obtained by discretising Hamilton's equations of motion. Finally, a finite difference method is developed in [3], also allowing the simulation of a stiff, damped string with an obstacle having an arbitrary shape. The case of the interaction between a string and a fretboard is in particular described in [17]. This obstacle is also considered in [18] where the Functional Transformation Method is used. However, in these models, eigenfrequencies and damping parameters cannot be arbitrary, but must follow a distribution specified by a small number of tuning parameters.

In this study, we present a conservative numerical scheme to model a stiff damped string vibrating against an arbitrarily shaped obstacle. The key features of the scheme are as follows. A modal expansion is used as a starting point for the linear case (i.e., in the absence of contact). By using an equal number of modes and discretization points, a linear transformation relates the spatial displacement and the modal coordinates, so that the contact force is treated directly with the displacement. Finally a regularized contact force together with an energy-conserving time-stepping scheme are implemented. Eigenfrequencies and damping parameters of the string can be adjusted at ease, and in particular according to experimental measurements so that sound synthesis can be more realistic.

Numerical results of the scheme are illustrated by considering two different obstacles for synthesizing the sounds produced by a string vibrating against a point obstacle and a distributed obstacle, mimicking the bridge of the tanpura and a flat bridge respectively. Sound examples are available at
www.lam.jussieu.fr/Membres/Issanchou/Sounds_DAFx16.html.

2. MODEL SYSTEM

Consider a stiff string of length L (m), tension T (N/m), and with linear mass density μ (kg/m). Stiffness effects in the string are characterised by Young's modulus E (Pa) of the material, and the moment of inertia $I = \pi r^4/4$, where r is the string radius, in m. The string vibrates in the presence of an obstacle assumed not in contact with the string at rest and described by a fixed profile $g(x)$, $x \in [0, L]$. See Figure 1. Under the assumption of small displacements, the dynamics of the string is described by the following equation of motion:

$$\mu u_{tt}(x,t) - T u_{xx}(x,t) + EI u_{xxxx}(x,t) = f(x,t), \quad (1)$$

where $u(x,t)$ is the transverse displacement of the string in a single polarisation perpendicular to the barrier. Partial differentiation with respect to time t and coordinate x are indicated by multiple subscripts. Simply supported boundary conditions at the string endpoints are assumed:

$$u(0,t) = u(L,t) = u_{xx}(0,t) = u_{xx}(L,t) = 0, \qquad \forall t \in \mathbb{R}^+. \quad (2)$$

No damping is considered as yet, and a detailed model of loss will be introduced once modal analysis has been perfomed. See Section 3.1.

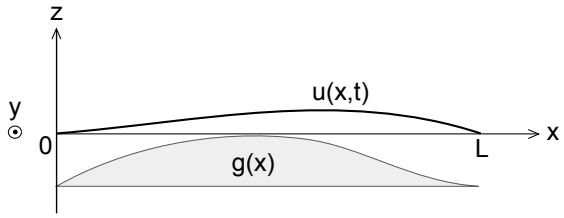

Figure 1: *A string of length L vibrating against an obstacle $g(x)$.*

$f(x,t)$ represents the contact force of the barrier upon the string. In general, it should be positive at times and locations along the string for which the string and barrier are in contact. A power-law expression is selected for the contact force. This choice has already been shown to be successful in the realm of musical acoustics [3, 17, 16, 19, 20]. The interaction force thus reads:

$$f(x,t) = f(\eta(x,t)) = K\left[\eta(x,t)\right]_+^\alpha, \tag{3}$$

where $\alpha \geq 1$ is a constant value, $\eta(x,t) = g(x) - u(x,t)$ is a measure of interpenetration of the string into the barrier, and $[\eta]_+ = 0.5\left(\eta + |\eta|\right)$ is the positive part of η [3]. Such a power-law model of a repelling force due to a collision may be interpreted as a compression of the medium in the case of flexible objects (such as, e.g., a piano hammer [21]). In the present case, it is best thought of as a regularized (smooth) force penalising such interpenetration [22]. As such, the constant K ideally will take on a very large value. This regularized approach contrasts with nonsmooth methods for which no penetration is allowed [23, 24].

One particular advantage of the present choice relies in the fact that the force f derives from a potential ψ:

$$f = \frac{d\psi}{d\eta}, \quad \text{with} \quad \psi(\eta) = \frac{K}{\alpha+1}\left[\eta\right]_+^{\alpha+1}. \tag{4}$$

This property is of special interest in the design of energy-conserving numerical methods. See Section 3.3.

2.1. Energy Balance

Energy techniques play an important role in the construction of numerical methods for highly nonlinear systems, as in the present case of the string in contact with a barrier. For instance, it is used in the present case of distributed collisions in [3], in the case of finite difference schemes. The basic strategy is to associate, with a given numerical method, a numerical conserved or dissipated energy quantity, which is itself a positive semi-definite function of the state. As such, it can be used to bound the dynamics of the system, and to find sufficient numerical stability conditions.

The continuous energy expression associated with (1) is obtained by multiplying (1) by u_t and then employing integration by parts over the spatial domain. It may be written as:

$$\mathscr{H} = \int_0^L \left[\frac{\mu}{2}(u_t)^2 + \frac{T}{2}(u_x)^2 + \frac{EI}{2}(u_{xx})^2 + \psi\right] dx. \tag{5}$$

It satisfies $\mathscr{H} \geq 0$ and the following equality:

$$\frac{d\mathscr{H}}{dt} = 0, \tag{6}$$

implying that energy is conserved. The first three terms in the expression correspond to stored energy due to the effects of inertia, tension and stiffness, respectively. The final term denotes the energy stored in the collision mechanism. Note that, as losses have not yet been introduced, the system is Hamiltonian. When losses are introduced, one should expect a balance of the form

$$\frac{d\mathscr{H}}{dt} + \mathscr{Q} = 0, \tag{7}$$

for some function $\mathscr{Q}(t) \geq 0$, with the interpretation of power loss, implying that

$$0 \leq \mathscr{H}(t) \leq \mathscr{H}(0) \tag{8}$$

for $t \geq 0$. It is not easy to give a simple expression for $\mathscr{Q}$ in the case of realistic models of loss in strings, which are usually expressed in the frequency domain [14], and not in terms of a spatiotemporal PDE system. Thus our expression for power loss is postponed until a modal analysis has been carried out. See Section 3.1.

3. NUMERICAL SCHEME FOR A STRING VIBRATING AGAINST AN OBSTACLE

The main characteristics of the numerical scheme are the following:
1. An exact scheme for a lossy linear oscillator without obstacle, as described in in [19], is used as a building block.
2. Each mode of the string can be described, in isolation, with such an oscillator. Therefore we apply the exact scheme to each mode, ensuring a fine description of frequencies and losses, adjusted for each mode. Then we add a force term F (corresponding to a modal representation of f in equation (1)). At this point, we obtain an equation in terms the modal coefficients of u.
3. Taking as many modes as interior points of the spatial mesh, we can rewrite the equation on u directly, through Fourier transformation. Then the force term is expressed as in [3], in order to obtain a conservative scheme.

3.1. Modal analysis

The modal expansion for the displacement of the string is as follows:

$$u(x,t) = \sum_{j=1}^{\infty} q_j(t)\phi_j(x), \quad \text{with} \quad \phi_j(x) = \sqrt{\frac{2}{L}}\sin\left(\frac{j\pi x}{L}\right) \tag{9}$$

for simply supported boundary conditions.

Inserting the expansion of u in (1), one obtains:

$$\mu(\ddot{\mathbf{q}} + \mathbf{\Omega}^2\mathbf{q}) = \mathbf{F}, \tag{10}$$

where $\mathbf{q}$ is a vector containing modal coefficients, and $\mathbf{\Omega}$ is a diagonal matrix such that $\Omega_{j,j} = \omega_j = 2\pi\nu_j$.
Eigenfrequencies are given by $\nu_j = j\frac{c}{2L}\sqrt{1+Bj^2}$, where $B = \frac{\pi^2 EI}{TL^2}$ describes the inharmonicity created by taking into account the stiffness of the string. Finally the vector $\mathbf{F}$ represents the modal

projection of the contact force, with $F_j = \int_0^L f(x,t)\phi_j(x)\mathrm{d}x$.

Equation (10) describes a lossless string, where the linear part corresponds to the description of a lossless oscillator for each mode. Therefore, losses can now be introduced by associating each mode with a lossy oscillator. Then (10) becomes [19]:

$$\mu(\ddot{\mathbf{q}} + \mathbf{\Omega}^2\mathbf{q} + 2\mathbf{\Sigma}\dot{\mathbf{q}}) = \mathbf{F}, \tag{11}$$

where $\mathbf{\Sigma}$ is a diagonal matrix such that $\Sigma_{j,j} = \sigma_j$. A damping parameter σ_j is now associated to each modal equation, and can be tuned at ease in order to consider any frequency dependence.

Let us now introduce the theoretical model for losses proposed in [14], which will allow us to determine realistic values to damping parameters in (11). This model takes into account the three main dissipation mechanisms in musical strings, namely friction with surrounding air, viscoelastic and thermoelastic behaviour of the material as internal losses. The following expression of the quality factor $Q_j = \frac{\pi\nu_j}{\sigma_j}$ has been given as:

$$Q_j^{-1} = Q_{j,air}^{-1} + Q_{j,ve}^{-1} + Q_{te}^{-1}, \tag{12}$$

where subscripts ve and te refer to viscoelastic and thermoelastic losses, and:

$$Q_{j,air}^{-1} = \frac{R}{2\pi\mu\nu_j},\ R = 2\pi\eta_{air} + 2\pi d\sqrt{\pi\eta_{air}\rho_{air}\nu_j},$$
$$Q_{j,ve}^{-1} = \frac{4\pi^2\mu EI\delta_{ve}}{T^2}\nu_j^2.$$

In these expressions, η_{air} and ρ_{air} are, respectively, the dynamic viscosity coefficient and the air density. In the rest of the paper, they are set to the following values, assumed constant: $\eta_{air} = 1.8 \times 10^{-5}$ kg m^{-1}s^{-1} and $\rho_{air} = 1.2$ kg m^{-3}. Finally this loss model depends on two parameters that can be fitted from e.g. experimental measurements, as performed for example in [14, 25, 20]: the viscoelastic losses angle δ_{ve}, and the constant value Q_{te}^{-1} characterizing the thermoelastic damping. It results in a frequency-dependent loss model which accurately takes into account the damping mechanism present in musical string vibrations [14, 25, 20].

3.2. Spatial discretization

The spatial discretization is defined as $x_i = \frac{iL}{N}$, $i \in \{0, ..., N\}$. Boundary conditions are $u(x_0, t) = 0$ and $u(x_N, t) = 0\ \forall t \in \mathbb{R}^+$. In the following, only the values of u on the grid with $i \in \{1, 2, ..., N-1\}$ are thus needed in any calculation.

Considering $N-1$ modes, the following relationship is fulfilled, $\forall i \in \{1, 2, ..., N-1\}$:

$$u_i(t) = \sum_{j=1}^{N-1} q_j(t)\phi_j(x_i) = \sum_{j=1}^{N-1} q_j(t)\sqrt{\frac{2}{L}}\sin\left(\frac{j\pi i}{N}\right). \tag{13}$$

This can be written in matrix form as $\mathbf{u} = \mathbf{S}\mathbf{q}$, where $S_{i,j} = \phi_j(x_i), \forall (i,j) \in \{1, ..., N-1\}^2$. The inverse of $\mathbf{S}$ can easily be calculated: $\mathbf{S}^{-1} = \frac{L}{N}\mathbf{S}^T$. This linear relation between $\mathbf{u}$ and $\mathbf{q}$ will be useful in the following analysis.

3.3. Time discretization

Some notations are first introduced:

$$u_i^n = u(n\Delta t, x_i)$$
$$\delta_{t-}\mathbf{u}^n = \frac{\mathbf{u}^n - \mathbf{u}^{n-1}}{\Delta t}$$
$$\delta_{t+}\mathbf{u}^n = \frac{\mathbf{u}^{n+1} - \mathbf{u}^n}{\Delta t}$$
$$\delta_{t\cdot}\mathbf{u}^n = \frac{\mathbf{u}^{n+1} - \mathbf{u}^{n-1}}{2\Delta t}$$
$$\delta_{tt}\mathbf{u}^n = \frac{\mathbf{u}^{n+1} - 2\mathbf{u}^n + \mathbf{u}^{n-1}}{\Delta^2}$$
$$\langle \mathbf{u}, \mathbf{v} \rangle = \Delta x \sum_{j\in\{1,\dots,N-1\}} u_j v_j.$$

Let us now consider the following time discretization of (11):

$$\frac{\mu}{\Delta t^2}(\mathbf{q}^{n+1} - \mathbf{C}\mathbf{q}^n + \tilde{\mathbf{C}}\mathbf{q}^{n-1}) = \mathbf{F}^n, \tag{14}$$

where $\mathbf{C}$, $\tilde{\mathbf{C}}$ are diagonal matrices such that :

$$C_{i,i} = e^{-\sigma_i\Delta t}\left(e^{\sqrt{\sigma_i^2-\omega_i^2}\Delta t} + e^{-\sqrt{\sigma_i^2-\omega_i^2}\Delta t}\right)$$
$$\tilde{C}_{i,i} = e^{-2\sigma_i\Delta t}.$$

When the contact force is not present, the modal approach may be viewed as an assembly of independent linear oscillators. This temporal integration scheme gives an exact solution in this case, as shown for example in [19], ensuring that at least the linear part is well-approximated (indeed, perfectly). The contact force, through which modes are coupled, remains to be determined. In order to avoid the difficulty linked to this coupling, the dynamical equation for the modal displacements vector $\mathbf{q}$ is rewritten for the physical displacement vector $\mathbf{u}$. Thanks to the linear relationship stated above between $\mathbf{u}$ and the modal displacement $\mathbf{q}$, the discrete equation on u can be written as:

$$\frac{\mu}{\Delta t^2}(\mathbf{u}^{n+1} - \mathbf{D}\mathbf{u}^n + \tilde{\mathbf{D}}\mathbf{u}^{n-1}) = \mathbf{f}^n, \tag{15}$$

where $\mathbf{D} = \mathbf{S}\mathbf{C}\mathbf{S}^{-1}$ and $\tilde{\mathbf{D}} = \mathbf{S}\tilde{\mathbf{C}}\mathbf{S}^{-1}$. The contact force expression used in the present approach is the same as in [3]: $\mathbf{f}^n = -\frac{\delta_{t-}\psi^{n+\frac{1}{2}}}{\delta_{t\cdot}\mathbf{u}^n}$, where $\psi^{n+\frac{1}{2}} = \frac{1}{2}(\psi^{n+1} + \psi^n)$ and $\psi^n = \psi(\eta^n)$. This formulation allows for a conservative scheme when there is no loss, and a dissipative one otherwise.

Therefore, at each time step, the following equation must be solved:

$$\mathbf{r} + \mathbf{b} + m\frac{\psi(\mathbf{r}+\mathbf{a}) - \psi(\mathbf{a})}{\mathbf{r}} = 0, \tag{16}$$

where $\mathbf{r} = \mathbf{u}^{n+1} - \mathbf{u}^{n-1}$ is the unknown, $\mathbf{a} = \mathbf{u}^{n-1}$, $m = \frac{\Delta t^2}{\mu}$ and $\mathbf{b} = -\mathbf{D}\mathbf{u}^n + \tilde{\mathbf{D}}\mathbf{u}^{n-1} + \mathbf{u}^{n-1}$. The Newton-Raphson algorithm may be used to this end [3].

Compared to a finite difference approach, the major advantage is the consideration of damping parameters and frequencies that can be adjusted mode by mode. However, the matrices $\mathbf{D}$, $\tilde{\mathbf{D}}$ are full in the modal case, as opposed to sparse in the case of local finite difference approximations, and computation time increases accordingly (see section 4.2).

Numerical energy analysis and stability conditions for the scheme are provided in the next section.

3.4. Stability analysis

The numerical scheme (15) is in a form close to actual implementation. However, in order to derive the discrete energy associated to the scheme, it is more convenient to rewrite it in terms of discrete temporal operators. Following the given in the case of an oscillator in [19] to get an equivalent scheme, one obtains:

$$\mu \left[\check{\mathbf{C}}_\mathbf{1} \delta_{tt} \mathbf{q}^n + \check{\mathbf{C}}_\mathbf{2} \mathbf{q}^n + \check{\mathbf{C}}_\mathbf{3} \delta_{t.} \mathbf{q}^n \right] = \mathbf{F}^n, \tag{17}$$

with $\check{\mathbf{C}}_\mathbf{1}$, $\check{\mathbf{C}}_\mathbf{2}$ and $\check{\mathbf{C}}_\mathbf{3}$ diagonal matrices satisfying:

$$\check{C}_{1_{ii}} = \frac{1 + (1-\gamma_i)\frac{\omega_i^2 \Delta t^2}{2}}{1 + (1-\gamma_i)\frac{\omega_i^2 \Delta t^2}{2} + \sigma_i^* \Delta t}$$

$$\check{C}_{2_{ii}} = \frac{\omega_i^2}{1 + (1-\gamma_i)\frac{\omega_i^2 \Delta t^2}{2} + \sigma_i^* \Delta t}$$

$$\check{C}_{3_{ii}} = \frac{2\sigma_i^*}{1 + (1-\gamma_i)\frac{\omega_i^2 \Delta t^2}{2} + \sigma_i^* \Delta t}.$$

The coefficients γ_i and σ_i^* may be written as

$$\gamma_i = \frac{2}{\omega_i^2 \Delta t^2} - \frac{A_i}{1 + e_i - A_i}$$

$$\sigma_i^* = \left(\frac{1}{\Delta t} + \frac{\omega_i^2 \Delta t}{2} - \gamma_i \frac{\omega_i^2 \Delta t}{2} \right) \frac{1 - e_i}{1 + e_i}$$

where

$$A_i = e^{-\sigma_i \Delta t} \left(e^{\sqrt{\sigma_i^2 - \omega_i^2} \Delta t} + e^{-\sqrt{\sigma_i^2 - \omega_i^2} \Delta t} \right) \text{ and } e_i = e^{-2\sigma_i \Delta t}. \tag{18}$$

The scheme for the displacement u thus may be written as:

$$\mu \left[\check{\mathbf{D}}_\mathbf{1} \delta_{tt} \mathbf{u}^n + \check{\mathbf{D}}_\mathbf{2} \mathbf{u}^n + \check{\mathbf{D}}_\mathbf{3} \delta_{t.} \mathbf{u}^n \right] = \mathbf{f}^n, \tag{19}$$

where $\check{\mathbf{D}}_\mathbf{1} = \mathbf{S}\check{\mathbf{C}}_\mathbf{1}\mathbf{S}^{-1}$, $\check{\mathbf{D}}_\mathbf{2} = \mathbf{S}\check{\mathbf{C}}_\mathbf{2}\mathbf{S}^{-1}$ and $\check{\mathbf{D}}_\mathbf{3} = \mathbf{S}\check{\mathbf{C}}_\mathbf{3}\mathbf{S}^{-1}$. The force term is expressed as previously.

A discrete energy balance can be obtained by taking the inner product between equation (19) and $\delta_{t.}\mathbf{u}^n$:

$$\delta_{t-} \mathbf{H}^{n+\frac{1}{2}} = -\mu \left\langle \delta_{t.} \mathbf{u}^n, \check{\mathbf{D}}_\mathbf{3} \delta_{t.} \mathbf{u}^n \right\rangle. \tag{20}$$

where :

$$\mathbf{H}^{n+\frac{1}{2}} = \frac{\mu}{2} \left\langle \delta_{t+} \mathbf{u}^n, \check{\mathbf{D}}_\mathbf{1} \delta_{t+} \mathbf{u}^n \right\rangle + \frac{\mu}{2} \left\langle \mathbf{u}^{n+1}, \check{\mathbf{D}}_\mathbf{2} \mathbf{u}^n \right\rangle + \left\langle \psi^{n+\frac{1}{2}}, 1 \right\rangle. \tag{21}$$

$\check{\mathbf{D}}_\mathbf{3}$ is positive semi-definite, so that the scheme is strictly dissipative. Therefore it is stable if the energy is positive.

Since the force potential is non-negative, the stability condition is given by:

$$\left\langle \delta_{t+} \mathbf{u}^n, (\check{\mathbf{D}}_\mathbf{1} - \frac{\Delta t^2}{4} \check{\mathbf{D}}_\mathbf{2}) \delta_{t+} \mathbf{u}^n \right\rangle \geq 0. \tag{22}$$

It is therefore sufficient to have $(\check{\mathbf{D}}_\mathbf{1} - \frac{\Delta t^2}{4} \check{\mathbf{D}}_\mathbf{2})$ positive semi-definite, which is true if $(\check{\mathbf{C}}_\mathbf{1} - \frac{\Delta t^2}{4} \check{\mathbf{C}}_\mathbf{2})$ is positive semi-definite. Consequently, the condition that must be satisfied may be written as:

$$\frac{1 + e_i + A_i}{1 + e_i - A_i} \geq 0 \; \forall i. \tag{23}$$

Equation (23) is satisfied if $1 + e_i \pm A_i > 0$.This is always true, and hence the scheme is unconditionally stable. The same conclusion is obtained in the limiting case $\sigma_i = 0 \; \forall i$, using the same reasoning leading to 22 with a reduced expression of γ_i.

3.5. Contact losses

Nonlinear losses due to contact can be added in the presented framework, following the considerations developed in [26, 3]. The contact force given by (3) may be modified as:

$$f = \frac{d\psi}{d\eta} - \frac{du}{dt} K \beta [\eta]_+^\alpha, \tag{24}$$

with $\beta \geq 0$.

The energy (5) of the system (with no loss inherent to the string) then satisfies [3]:

$$\frac{d\mathscr{H}}{dt} = -\mathscr{Q}_{contact} \tag{25}$$

where

$$\mathscr{Q}_{contact} = \int_0^L (u_t)^2 K \beta [\eta]_+^\alpha dx. \tag{26}$$

The additional damping term may be discretised using the following expression [3]: $\delta_{t.}\mathbf{u}^n K \beta [\eta^n]_+^\alpha$.

Instead of (16), the equation to be solved at each time step is then:

$$(1 + c)\mathbf{r} + \mathbf{b} + m \frac{\psi(\mathbf{r} + \mathbf{a}) - \psi(\mathbf{a})}{\mathbf{r}} = 0, \tag{27}$$

where $c = \frac{\Delta t}{2\mu} K \beta [\mathbf{g} - \mathbf{u}^n]_+^\alpha$. The discrete energy balance is given by:

$$\delta_{t-} \mathbf{H}^{n+\frac{1}{2}} = -\mu \left\langle \delta_{t.} \mathbf{u}^n, \check{\mathbf{D}}_\mathbf{3} \delta_{t.} \mathbf{u}^n \right\rangle - \left\langle \delta_{t.} \mathbf{u}^n, \delta_{t.} \mathbf{u}^n K \beta [\eta^n]_+^\alpha \right\rangle. \tag{28}$$

Since $\langle \delta_{t.} \mathbf{u}^n, \delta_{t.} \mathbf{u}^n K \beta [\eta^n]_+^\alpha \rangle \geq 0$, the dissipation in the system is then increased.

4. APPLICATION TO MUSICAL INSTRUMENTS AND SOUND SYNTHESIS

In this section, the numerical scheme presented previously is used to simulate the motion of a string vibrating against an obstacle. The cases of a point obstacle and a distributed obstacle are considered.

The string to be considered here is of length $L = 1.002$ m, under tension $T = 180.5$ N and with linear mass density $\mu = 1.17 \times 10^{-3}$ kg/m. Musical strings are known to have a very small stiffness. Consequently, the inharmonicity coefficient B introduced in Section 3.1 is chosen to be $B = 1.78 \times 10^{-5}$, corresponding to measured values according to the protocol described in [20]. In order to show the ability of the model to incorporate a complex damping law, the theoretical loss model introduced in section 3.1 is used. The values $\delta_{ve} = 0.0045$ and $Q_{te}^{-1} = 0.000203$ have been chosen, and correspond to experimental data, obtained using the method exposed in [20]. This model has a complex frequency dependence and accounts for the main loss mechanisms present in strings.

First, a time step, or sample rate has to be chosen. To this end, a convergence study has been undertaken, as elaborated in the following section.

4.1. Convergence study

Contact problems lead to the spontaneous generation of high frequencies in the system, due to the very short timescales resulting from collisions between very stiff objects, as in the present case. This implies, at least in theory, a need for a high sampling rate in order to obtain accurate results, which should decrease as the contact stiffness does. The presence of damping, particularly at high frequencies, is expected to be an ameliorating factor. In order to highlight such accuracy issues, as they relate to the time step, convergence results are presented here.

Consider a point obstacle located at $x = 6$ mm (see Section 4.3). In Figure 2, time history and spectrograms of simulation output are shown, where output is taken as the velocity at the bridge. For the contact restoring force, $K = 10^{13}$ and $\alpha = 1.3$ in order to obtain a stiff contact, limiting penetration of the string in the obstacle to the range of 1×10^{-8} m. With $K = 10^9$ for instance, the penetration attains about 1×10^{-5} m and the resulting sound richness is significantly altered. The string is initially plucked at $x = L/2$, with a maximal displacement of 1.8 mm.

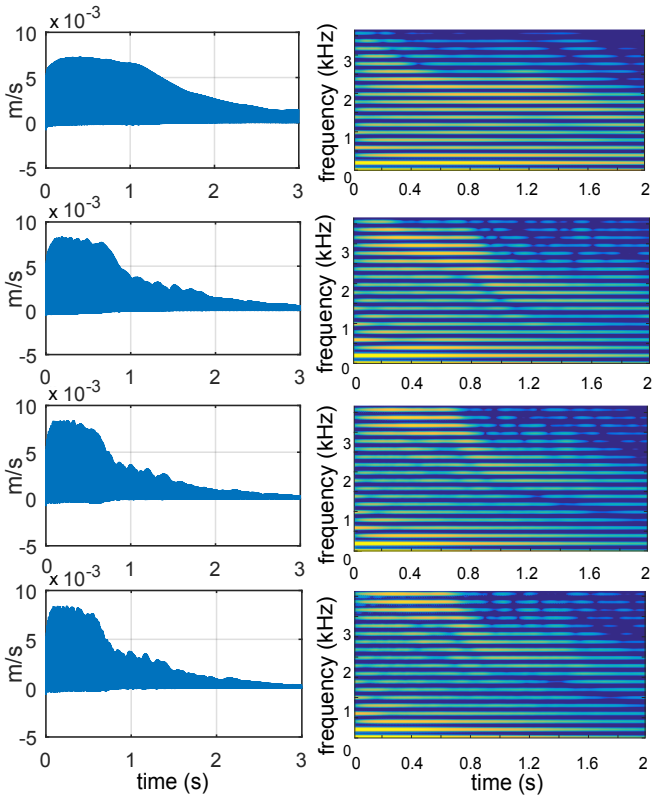

Figure 2: *At left : time-domain output signals. At right : spectrograms. From top to bottom :* $F_s = 128, 256, 512$ *and* 1024 *kHz.*

Figure 2 clearly highlights that for a sample rate $F_s = 1/\Delta t = 128$ kHz, the simulated sound is far from convergence (it is substantially different from the result with $F_s = 1024$ kHz), and thus not reliable. From $F_s = 256$ kHz, the general shape of the time history, together with the spectral dynamics, seems to be correctly reproduced. However, detailed view inside the signal and auditory comparisons definitely evidenced that the high frequencies components are not well reproduced, such that this sample rate is still insufficient. Finally, careful inspection crossed with listening tests shows that a sample rate of at least $F_s = 1$ MHz is necessary for convergence of numerical results. To be confident with the accuracy of the simulations presented below, the sampling rate has been fixed for all the simulations to $F_s = 2$ MHz. Note also that careful comparisons with experimental results have been presented in [20], for which a sample rate of 2 MHz was also necessary to obtain very satisfactory results over long simulation times.

4.2. Computation cost

In this part, computation times of the numerical scheme are discussed. The computations have been realized with MATLAB on a single CPU with a clock at 2.4 GHz, and time costs are given in table 1 for the computation of one second of sound, rounded up to the nearest minute when $N = 1001$. Steps which are controlled are the Newton-Raphson loop, the computation of $\mathbf{b}, \mathbf{a}, \mathbf{r}^n$ in (16), the computation of the energy given in (21) and finally the total time is given. It clearly appears that the most costly steps are

$N-1=500$				
F_s	44.1 kHz	88.2 kHz	176 kHz	1 MHz
Newton-Raphson	0.7	1.3	2.6	9.8
$\mathbf{b}, \mathbf{a}, \mathbf{r}^n$ in (16)	1.5	3.1	6	31.4
Energy	0.8	1.7	3.5	16.8
Total time	3.1	6.4	12.5	59.5
$N-1=1001$				
F_s	44.1 kHz	88.2 kHz	176 kHz	1 MHz
Newton-Raphson	1	2	4	14
$\mathbf{b}, \mathbf{a}, \mathbf{r}^n$ in (16)	5	7	14	119
Energy	3	6	12	54
Total time	10	16	30	189

Table 1: *Computation times, in minutes, for* $N - 1 = 500$ *and* $N - 1 = 1001$.

the computation of $\mathbf{b}, \mathbf{a}, \mathbf{r}^n$ and the energy, i.e. products of matrices and vectors, most probably because involved matrices are full. Therefore, the computation time is mostly driven by N, so that a judicious way of reducing computation cost may be to adapt the spatial grid to the obstacle, making the space grid finer around the obstacle and larger elsewhere.

4.3. Point obstacle: case of the tanpura

The tanpura is an Indian instrument which is played by plucking open strings. The strings are connected to a curved bridge over which a thread is carefully installed makes the sound very specific to this instrument. This bridge and its thread (fully modelled in [15]) can mostly be described as a two point bridge [14]. Therefore in this part, this two point bridge is considered: assuming that the bridge is at $x = 0$, a point obstacle is located at $x = 6$ mm. Two initial conditions are considered, by plucking the string at $x = L/5$ and $x = 4L/5$, and the velocity of the string is computed at the bridge.

Parameters of the contact force are $K = 10^{13}$ and $\alpha = 1.3$ as in Section 4.1, and the spatial grid is such that $N = 1001$. At the initial time a smoothed triangle with a maximal amplitude of about 1 mm is imposed as the initial displacement, with no velocity. This small value has been chosen in order to show that even for very

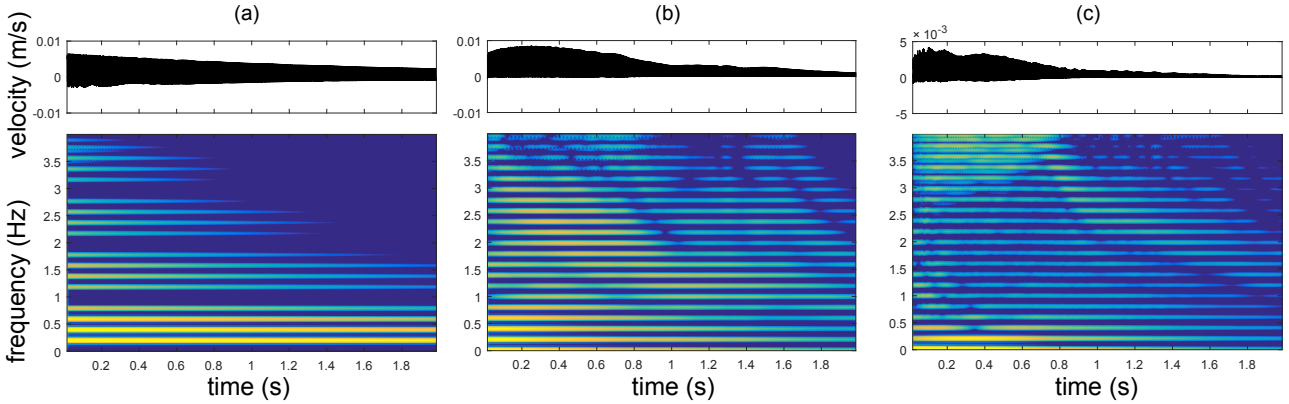

Figure 3: *Spectral evolution of velocities at the bridge (a) no obstacle, plucking at $x = L/5$ (b) point obstacle, plucking at $x = L/5$ (c) point obstacle, plucking at $x = 4L/5$.*

small displacements, the contact can introduce strong nonlinear effects which are clearly audible and visible on signals.

When there is no obstacle, one can observe rejection of modes which are not excited by the initial condition, as well as a faster damping of high frequencies compared to low frequencies (see Figure 3). When the obstacle is added, all modes are present and energy is transmitted from modes to others. Spectrum tendencies are similar to those encountered in [15] (numerical results) and [14] (experimental results).

The velocity signal for the string with an obstacle is mostly positive (see Figure 4), this is due to the close position of the measure position to the obstacle. Moreover, the effect of the string stiffness implies dispersion which is clearly visible on temporal signals, and constitutes a precursor. When the plucked point is at $x = 4L/5$ rather than $x = L/5$, the precursor needs more time to reach the obstacle, therefore it is much more developed when arriving, which explains the high frequencies richness of the temporal signal in Figure 4.

Moreover, according to [14], the frequency sliding depends on the plucking position, which is also observed here.

The temporal evolution of energy $\mathbf{H}^{n+\frac{1}{2}}$ is presented in Figure 5. It decreases faster when there is an obstacle, probably because energy is transmitted to higher modes, which are more damped. For a plucking point at $x = 4L/5$, the energy decreases faster than at $x = L/5$, since more high frequencies are generated by the bridge.

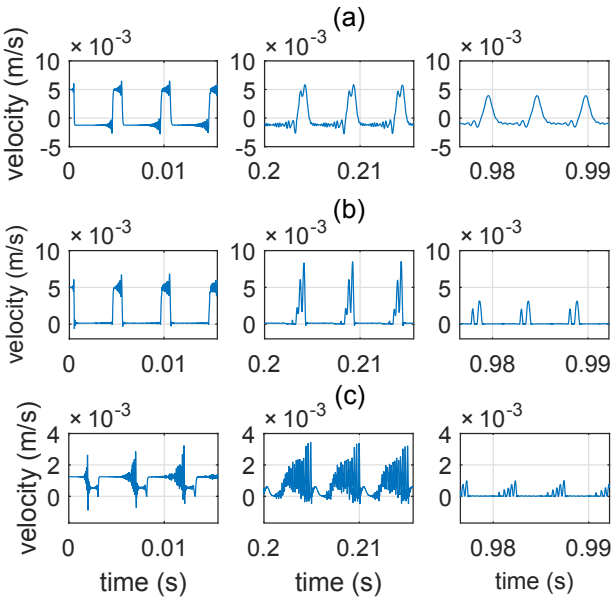

Figure 4: *Temporal evolution of velocities at the bridge for a point obstacle mimicking the case of the tanpura (a) no obstacle, plucking at $x = L/5$ (b) point obstacle, plucking at $x = L/5$ (c) point obstacle, plucking at $x = 4L/5$*

4.4. Distributed obstacle

In this part, a distributed parabolic obstacle is considered at one end of the string, that could mimic the case of a sitar. Its shape is as follows:

$$g(x) = -ax^2, \tag{29}$$

where we set $a = 0.0065$. The length of the obstacle is 19 mm (see Figure 6). Such a value, small compared to realistic ones (see for instance [13], where a measure gives $a = 0.5778$), is chosen in order to make the contact between the string and the full length of the bridge arise. No particular adjustment is made in terms of inclination, however interesting observations can already be made.

Numerical parameters K, α and the initial condition are the same as previously. Temporal and spectral evolutions are presented in Figures 7 and 8, as well as the energy of the signal. Because of the obstacle, the velocity signal at the bridge as a minimum value close to 0.

Similarly to the case of the point obstacle, a precursor is visible from the first periods and high frequencies are highly excited by the contact, which results in narrow peaks on temporal signals (Figure 7). As mentioned in [12] for experimental results on a complete instrument, the absence of rejection and a descending formant can clearly be observed in Figure 8. Moreover, as in the point obstacle case, the energy decrease is faster than when there is no obstacle, which may be due to the transfer of energy from lower to higher modes, combined with larger damping at high frequencies.

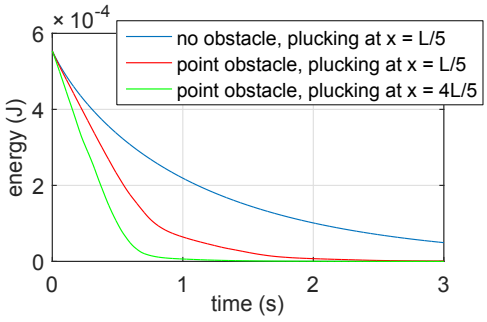

Figure 5: *Energy decay for different configurations.*

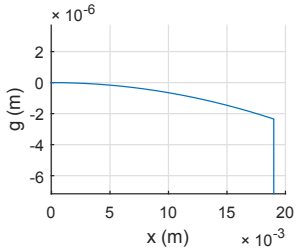

Figure 6: *Shape of the distributed obstacle.*

5. CONCLUSION

A numerical method combining a modal approach and an energy-conserving scheme for the case of the string in contact with a barrier has been introduced. Due to the modal approach, the linear parameters of the strings (eigenfrequencies and damping coefficients) can be set independently for each mode, allowing for flexible control over frequency-dependent loss. In particular, linear characteristics of a measured string can be used in order to obtain very realistic sounds, as proposed in [20]. Such complete control over damping rates for the string constitutes one of the major advantages of a modal approach to synthesis. The scheme itself, though with modal characteristics, operates ultimately in the spatial domain, much like a finite difference scheme, though with the special property of being exact under linear conditions. Such a method can thus be viewed as a type of spectral method [27], accompanied by a time-stepping method which is tuned according to the modal frequencies (unlike, e.g., more typical methods such as leap-frog, or members of the Runge-Kutta family). As with spectral methods, though the updates are no longer sparse, as in the case of FD schemes, it may be possible to employ fast transforms (such as a variant of the FFT) in order to perform the updates (which in this case, follows directly from the sinusoidal structure of the matrix $\mathbf{S}$).

It has been shown that a high sample rate is necessary in order to obtain reliable results for simulations over a long duration. Computation time, which does not allow a real-time simulation at present on a standard machine, could be improved by considering a variable spatial step, finer in the region surrounding the obstacle, and possibly a variable time step [28], since high temporal precision is only necessary when the string is in contact with the obstacle. In audio applications, though, such algorithmic refinements must be treated with care—the use of a variable grid spacing

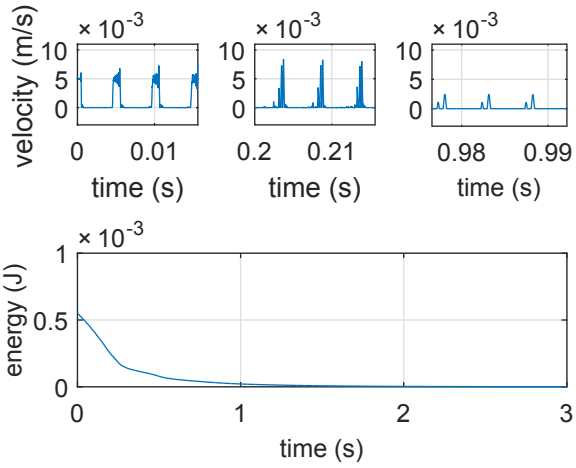

Figure 7: *Temporal evolution of the velocity at the bridge and its energy*

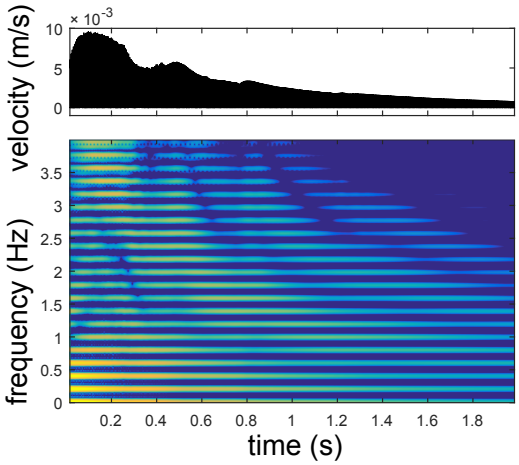

Figure 8: *Spectral evolution of the velocity at the bridge, distributed obstacle*

will entail a loss of structure in the resulting update matrices, and the use of a variable time step must necessarily be accompanied by some form of on-line sample rate conversion which is perceptually transparent.

The next steps of this research will consider more closely the comparison between the outcomes of these numerical methods and measurements realized on a real string and/or on real instruments. To this end, and also in the interest of higher quality synthesis, a parametric study on the contact force parameters should be carried out, and the incorporation of various additional features of the string/barrier system would be of interest. One such feature is the extension of string vibration to two polarisations, as recently explored in the context of bowed string synthesis [29] and in case of the tanpura [30]. At present, there is not a model of an excitation mechanism, and a refined plucking model could be included, perhaps modeling the dynamics of the player's fingers [31]. Ultimately, a complete instrument will require a model of coupling to the instrument body, acoustic radiation, and possibly sympathetic strings [32].

6. ACKNOWLEDGMENTS

This work was supported by the European Research Council, under grant number ERC-2011-StG-279068-NESS.

7. REFERENCES

[1] X. Boutillon, "Model for piano hammers: Experimental determination and digital simulation," *J. Acoust. Soc. Am.*, vol. 83, no. 2, pp. 746–754, 1988.

[2] A. Chaigne, P. Joly, and L. Rhaouti, "Numerical modeling of the timpani," in *European Congress on Computational Methods in Applided Sciences and Engineering, Barcelona*, 2000.

[3] S. Bilbao, A. Torin, and V. Chatziioannou, "Numerical modeling of collisions in musical instruments," *Acta Acustica united with Acustica*, vol. 101, pp. 155–173, 2015.

[4] H. Cabannes, "Cordes vibrantes avec obstacles," *Acustica*, vol. 55, pp. 14–20, 1984.

[5] M. Schatzman, "A hyperbolic problem of second order with unilateral constraints: The vibrating string with a concave obstacle," *Journal of Mathematical Analysis and Applications*, vol. 73, pp. 138–191, 1980.

[6] R. Burridge, J. Kappraff, and C. Morshedi, "The sitar string, a vibrating string with a one-sided inelastic constraint," *SIAM Journal of Applied Mathematics*, vol. 42, no. 6, pp. 1231–1251, 1982.

[7] E. Rank and G. Kubin, "A waveguide model for slapbass synthesis," in *Acoustics, Speech, and Signal Processing, 1997. ICASSP-97., 1997 IEEE International Conference on*, 1997, vol. 1, pp. 443–446.

[8] G. Evangelista and F. Eckerholm, "Player-instrument interaction models for digital waveguide synthesis of guitar: Touch and collisions," *IEEE transactions on audio, speech, and language processing*, vol. 18, no. 4, pp. 822–832, 2010.

[9] D. Kartofelev, A. Stulov, H.-M. Lehtonen, and V. Välimäki, "Modeling a vibrating string terminated against a bridge with arbitrary geometry," in *Proceedings of the Stockholm Music Acoustics Conference*, 2013.

[10] D. Kartofelev, A. Stulov, and V. Välimäki, "Pitch glide effect induced by a nonlinear string-barrier interaction," in *AIP Conference Proceedings*, 2015.

[11] A. Krishnaswamy and J. O. Smith, "Methods for simulating string collisions with rigid spatial objects," in *Proc. IEEE Workshop of Applications of Signal Processing to Audio and Acoustics*, 2003, pp. 233–236.

[12] S. Siddiq, "A physical model of the nonlinear sitar string," *Archives of acoustics*, vol. 37, no. 1, pp. 73–79, 2012.

[13] C. P. Vyasarayani, S. Birkett, and J. McPhee, "Modeling the dynamics of a vibrating string with a finite distributed unilateral constraint: Application to the sitar," *J. Acoust. Soc. Am.*, vol. 125, no. 6, pp. 3673–3682, 2009.

[14] C. Valette and C. Cuesta, *Mécanique de la corde vibrante*, Hermès, 1993.

[15] V. Chatziioannou and M. van Walstijn, "Numerical simulation of tanpura string vibrations," *ISMA*, pp. 609–614, 2014, Le Mans, France.

[16] V. Chatziioannou and M. van Walstijn, "Energy conserving schemes for the simulation of musical instrument contact dynamics," *Journal of Sound and Vibration*, vol. 339, pp. 262–279, 2015.

[17] S. Bilbao and A. Torin, "Numerical simulation of string/barrier collisions: the fretboard," in *Int. Conference on Digital Audio Effects (DAFx-14)*, 2003.

[18] L. Trautmann and R. Rabenstein, "Multirate simulations of string vibrations including nonlinear fret-string interactions using the functional transformation method," *EURASIP Journal on Applied Signal Processing*, vol. 7, pp. 949–963, 2004.

[19] S. Bilbao, *Numerical Sound Synthesis: Finite Difference Schemes and Simulation in Musical Acoustics*, Wiley, 2009.

[20] C. Issanchou, S. Bilbao, O. Doaré, J.-L. Le Carrou, and C. Touzé, "Méthode modale mixte pour le contact unilatéral corde / obstacle : application au chevalet de la tampoura," in *Congrès Français d'Acoustique, Le Mans, France*, 2016.

[21] A. Chaigne and A. Askenfelt, "Numerical simulations of piano strings. i. a physical model for a struck string using finite difference methods," *J. Acoust. Soc. Am.*, vol. 95, no. 2, pp. 1112–1118, 1994.

[22] D. Harmon, "Robust, efficient, and accurate contact algorithms," PhD Thesis, Department of Computer Science, Columbia University, 2010.

[23] A. Banerjee, A. Chanda, and R. Das, "Historical origin and recent development on normal directional impact models for rigid body contact simulation: A critical review," *Archives of Computational Methods in Engineering*, pp. 1–26, 2016.

[24] B. Brogliato and V. Acary, *Numerical Methods for Nonsmooth Dynamical Systems. Applications in Mechanics and Electronics*, Springer Verlag, 2008.

[25] A. Paté, J.-L. Le Carrou, and B. Fabre, "Predicting the decay time of solid body electric guitar tones," *J. Acoust. Soc. Am.*, vol. 135, no. 5, pp. 3045–3055, 2014.

[26] K. Hunt and F. Crossley, "Coefficient of restitution interpreted as damping in vibroimpact," *J. Applied Mech.*, pp. 440–445, 1975.

[27] L. N. Trefethen, *Spectral Methods in MATLAB*, SIAM, 2000.

[28] P. Flores and J. Ambrósio, "On the contact detection for contact-impact analysis in multibody systems," *Multibody Syst Dyn*, vol. 24, pp. 103–122, 2010.

[29] C. Desvages and S. Bilbao, "Two-polarisation finite difference model of bowed strings with nonlinear contact and friction forces," in *Int. Conference on Digital Audio Effects (DAFx-15)*, 2015.

[30] J. Bridges and M. Van Walstijn, "Investigation of tanpura string vibrations using a two-dimensional time-domain model incorporating coupling and bridge friction," in *Proc. of the third Vienna Talk on Music Acoustics*, 2015.

[31] D. Chadefaux, J.-L. Le Carrou, and B. Fabre, "A model of harp plucking," *J. Acoust. Soc. Am.*, vol. 133, no. 4, pp. 2444–2455, 2013.

[32] J.-L. Le Carrou, F. Gautier, N. Dauchez, and J. Gilbert, "Modelling of sympathetic string vibrations," *Acta Acustica united with Acustica*, vol. 91, no. 2, pp. 277–288, 2005.